

## Image Fusion and Image Quality Assessment of Fused Images

**Manjusha Deshmukh**

*Saraswati college of Engg.,  
Navi Mumbai,  
410210, India,*

manju0810@yahoo.com

**Udhav Bhosale**

*Rajiv Gandhi Institute of Technology,  
Mumbai,  
India*

udhav.bhosle@gmail.com

---

### Abstract

Accurate diagnosis of tumor extent is important in radiotherapy. This paper presents the use of image fusion of PET and MRI image. Multi-sensor image fusion is the process of combining information from two or more images into a single image. The resulting image contains more information as compared to individual images. PET delivers high-resolution molecular imaging with a resolution down to 2.5 mm full width at half maximum (FWHM), which allows us to observe the brain's molecular changes using the specific reporter genes and probes. On the other hand, the 7.0 T-MRI, with sub-millimeter resolution images of the cortical areas down to 250  $\mu\text{m}$ , allows us to visualize the fine details of the brainstem areas as well as the many cortical and sub-cortical areas. The PET-MRI fusion imaging system provides complete information on neurological diseases as well as cognitive neurosciences. The paper presents PCA based image fusion and also focuses on image fusion algorithm based on wavelet transform to improve resolution of the images in which two images to be fused are firstly decomposed into sub-images with different frequency and then the information fusion is performed and finally these sub-images are reconstructed into result image with plentiful information. . We also propose image fusion in Radon space. This paper presents assessment of image fusion by measuring the quantity of enhanced information in fused images. We use entropy, mean, standard deviation and Fusion Mutual Information, cross correlation, Mutual Information Root Mean Square Error, Universal Image Quality Index and Relative shift in mean to compare fused image quality. Comparative evaluation of fused images is a critical step to evaluate the relative performance of different image fusion algorithms. In this paper, we also propose image quality metric based on the human vision system (HVS).

**Keywords:** Hotelling Transform, Wavelet Transform, Radon Transform, Image Registration, Image Fusion.

---

### 1. INTRODUCTION

Image fusion is useful technique for merging similar sensor and multi-sensor images to enhance the information. Modern imaging technologies visualize different aspects of disease in a non-invasive way. Considerable progress has been made in the fusion of images from different

imaging modalities using software approaches. One goal of fusion software is to align anatomical and functional images and allow improved spatial localization of abnormalities. Image fusion takes place at three different levels i.e. pixel, feature and decision. Image fusion methods can be broadly classified into two that is special domain fusion and transform domain fusion. Averaging, Brovery method, Principal Component Analysis (PCA), based methods are special domain methods. But special domain methods produce special distortion in the fused image .This problem can be solved by transform domain approach. The multi-resolution analysis has become a very useful tool for analyzing images. The discrete wavelet transform has become a very useful tool for fusion. The images used in image fusion should already be registered. Mis-registration is a major source of error in image fusion. Pixel level fusion technique is used to increase the special resolution of the multi-spectral image. Application of image fusion include improving geometric correction, enhancing certain features not visible in either of the single data alone, change detection using temporal data sets and enhancing provide a complete information for diagnosis.

Image fusion needs image registration. Choice of method of image registration depends on application. Goal of image registration is to find a transformation that aligns one image to another. In image registration, one dataset is regarded as the reference data and other as sensed data. Sensed data is matched relative to the reference data. A large number of automatic image registration methods have been proposed and surveys can be found in [1], [2], [ 3]. Image registration at a very basic level can be studied from [4].

P.A. Vanden Elsen et al. proposed that a single composite image from different modality images of the same subject and provide a complete information for diagnosis.[11]. H. Li, B.S. Manjunath and S. K. Mitra adopted wavelet transform for multisensor image fusion.[12]. Researchers also proposed that wavelet based fusion method retains and inherits the main merits of tower shaped transformation [13, 14]. David A.Y. proposed method for image merging by means of discrete two dimensional wavelet transform [15]. Mallat and Zhong proposed that if the wavelet coefficients undergo a modification like coefficient merging, quantization etc. then the inverse transform preserves this modification because the transform is non redundant [16]. Sveinsson et al. proposed cluster based feature extraction and data fusion in the wavelet domain [17]. Gorzelli explained possibilities and limitations to use wavelets in image fusion [18]. Lau Wai Leung et al compared image fusion techniques using entropy and image noise index (INI) [19]. Chavez et al. proposed three different methods to merge multiresolution and multispectral data [20]. Haim Schweitzer in his paper proposed that large collection of images can be indexed by projections on a few “ eigenfeatures “ , the dominant eigenvectors of the images covariance matrix [5]. Ma Debao and Liwagao introduced the new matrix characteristic methods like eigenvalues and eigenvectors and achievable accuracy is derived theoretically and verified by tests using simulated interferometric data.[9]. Wen Cao and Bicheng proposed PCAT (Principal Component Analysis Transform) and WPT (Wavelet Packet Transform) for remotely sensed image fusion [6]. Jiangsheng You, Weiguo Lu, Jian Li et. al. presented use of Radon transform for image matching [19]. Lau Wai Leung , Bruce King and Vijay Vohora compared image fusion techniques using entropy and INI [20]. Rockinger, O., proposed new merger based on shift invariant discrete wavelet transform(SIDWT) theory using maximum value selection rule of approximation coefficients for landslide characteristic enhancement [21]. Ramac, L. C., Uner, M. K., Varshney, P. K., presented Morphological filters and wavelet based image fusion. [22]. Nunez, J., proposed Multiresolution based image fusion with additive wavelet decomposition [23]. Alexander Toet, van Ruyven, J.J. & Valeton, J.M. introduced a hierarchical image merging scheme based on a multiresolution contrast decomposition i.e. the ratio of a low-pass pyramid[24]. Vivek Maik , Jeongho Shin and Joonki Paik Presented a pattern selective fusion method which provides a mechanism for combining multiple monochromatic images through identifying salient features in source images and combining those features into a single fused image[25]. Wen Doua, Yunhao Chen presented the relationships between image fusion methods aiming to reveal the nature of various methods[26]. Andrew P. Bradley proposed number of approaches to reducing, or removing, the problem of shift variance in the discrete wavelet transform (DWT) . They proposed over complete DWT (OCDWT) [27]. Milad Ghantous, Soumik Ghosh and Magdy Bayoumi

presented a hybrid image fusion scheme that combines features of pixel and region based fusion, to be integrated in a surveillance system [28]. Toet J. Ruvan and J. Valetton proposed image merging by contrast pyramid [29]. Alexander Toet presents a scheme to enhance image contrast by nonlinear multiplication of successive layers of the ROLP image decomposition [30]. P. Burt, E. Adelson proposed a Laplacian pyramid based approach for image fusion [31]. Xydeas, C., and Petrovic, V. assess pixel-level image fusion algorithms in their paper. [32].

This paper is organized as follows literature survey has been presented in section I, section II deals with fusion algorithms. Fused image evaluation methods have been presented in section III. Result is presented in section IV, We conclude in section V and bibliography has been presented in section VI.

## 2. FUSION ALGORITHMS

The details of PCA, Wavelet algorithm, Radon algorithm and their use in image fusion as well as simple average fusion algorithm are explained in this section. Experiments are carried out on following sample image.

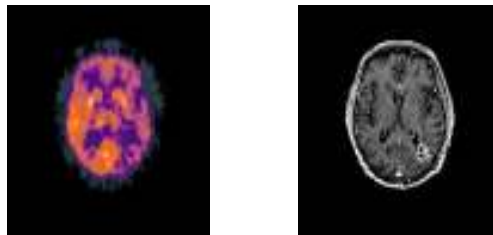


FIGURE 1: Sample images , PET (left ) and MRI (right).

### 2.1 Principal Component Analysis

Principal component analysis is one of the most frequently used dimension reduction method. Principal component analysis also called as Hotelling Transform [15]. If we have 'n' component images having different pixel values, these images can be treated as a unit by expressing each group of 'n' corresponding pixels as a vector, for eg. , let  $x_1, x_2, \dots, x_n$  are values of first pixel in each of the 'n' images then 'n' elements can be expressed as follows

$$x = \begin{bmatrix} x_1 \\ x_2 \\ \vdots \\ x_n \end{bmatrix} \quad \text{---} \quad \langle 1 \rangle$$

Where, x is column vector. This one vector represents one common pixel in all two images. If images are of size  $P \times Q$ , there will be total of  $N=P*Q$  such n- dimensional vectors. We can assume these vectors as random quantities, Mean vector of population is

$$m_x = E[x] \quad \text{---} \quad \langle 2 \rangle$$

The covariance matrix of vector population is

$$C_x = E\{(x - m_x)(x - m_x)^T\} \quad \text{---} \quad \langle 3 \rangle$$

Element  $C_{ij}$  of  $C_x$  is the variance of  $x_i$ , the  $i^{\text{th}}$  component of X vectors and element  $C_{ij}$  is covariance between components  $x_i$  and  $x_j$ . The matrix  $C_x$  is symmetric and real. For a sample of

N vectors from a random population, the mean vector and covariance matrix can be given by expression

$$m_x = \left(\frac{1}{N}\right) \sum_{k=1}^N x_k \text{ -----(4)}$$

Thus covariance matrix can be estimated as

$$C_x = \left(\frac{1}{N}\right) \sum_{k=1}^N x_k x_k^T - m_x m_x^T \text{ -----(5)}$$

Since  $C_x$  is real and symmetric, it is possible to find a set of N ortho-normal eigenvectors. Let  $e_i$  and  $\lambda_i$  be eigenvectors and corresponding eigenvalues of  $C_x$  where  $i = 1, 2, \dots, N$ . 'A' is a matrix whose rows are eigenvectors of covariance matrix  $C_x$ . Then A is ordered so that the first row of A is eigenvectors corresponding to the largest eigenvalue, and last row correspond its smallest eigenvalue. If we use A as transformation matrix to map the x's into y. Then y is given by

$$Y = A(x - m_x) \text{ -----(6)}$$

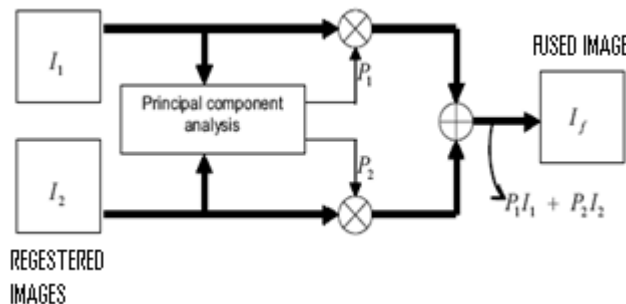
Above expression of 'y' is called Hotelling Transform or Principal Component Transform . Alternatively, the Hotelling Transform can be viewed as the discrete version of the Karbunen-Loeve transform (KLT)[4].

**A. PCA Algorithm**

The most straightforward way to build a fused image of several input images is performing the fusion as a weighted superposition of all input images. The optimal weighting coefficients, with respect to information content and redundancy removal, can be determined by a principal component analysis (PCA) of all input intensities. By performing a PCA of the covariance matrix of input intensities, the weightings for each input image are obtained from the eigenvector corresponding to the largest eigenvalue.

Arrange source images in two-column vector.

- Organize the data into column vector. Let S is the resulting column vector of dimension 2 X n.
- Compute empirical mean along each column. The empirical mean vector Me has a dimension 1 X 2.
- Subtract Me from each column of S. The resulting matrix X has dimension 2 X n.
- Find covariance matrix C of matrix X. Mean expectation will be equal to covariance of X.
- Compute eigenvectors and eigenvalue and sort them by decreasing eigenvalue.
- Consider first column of eigenvector which correspond to larger eigenvalue to compute normalized component  $P_1$  and  $P_2$ .



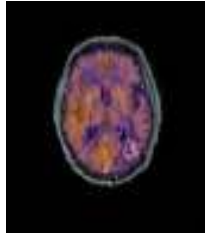


**FIGURE 2:** Image fusion scheme employing PCA and fused image

**Image Fusion based on Wavelet Decomposition**

Wavelet transform decomposes an image into various sub images based on local frequency content. Using discrete wavelet transform (DWT), a function  $f(t)$  can be represented by

$$f(t) = \sum_{j,k} a_{j,k} \psi_{jk}(t) \dots \dots \dots \langle 7 \rangle$$

Where  $a_{j,k}$  are wavelet coefficients,  $\psi_{j,k}(t)$  are basis function,  $j$  is scale,  $k$  is translation of mother wavelet  $\psi(t)$ . Two dimensional DWT can be obtained by applying DWT across rows and columns of an image. The two dimensional DWT of image  $f(x,y)$  is

$$f(x,y) = \sum_{j,k} C_{J_0}(k,l) \phi_{j,k,l}(x,y) + \sum_{S=H,V,D} \sum_{J=J_0}^{\infty} \sum_{k,l} D_j^S[k,l] \psi_{j,k,l}^S(x,y) \dots \dots \dots \langle 8 \rangle$$

Where  $C_{J_0}$  is approximation coefficient,  $\phi_{j,k,l}(x,y)$  is scaling function,  $D_j^S$  is set of detail coefficients and  $\psi_{j,k,l}$  is set of wavelet function

The DWT coefficients are computed by using a series of low pass filter  $h[k]$ , high pass filters  $g[k]$  and down samplers across both rows and columns. The results are the wavelet coefficient the next scale. The filter bank approach to calculate two dimensional dyadic DWT is shown in figure 3 and dyadic representation of the DWT is shown in figure 4. The wavelet coefficients are of smaller spatial resolution as they go from finer scale to coarser scale. The coefficients are called the approximation (A), horizontal detail (H), vertical detail (V) and diagonal detail (D) coefficient.

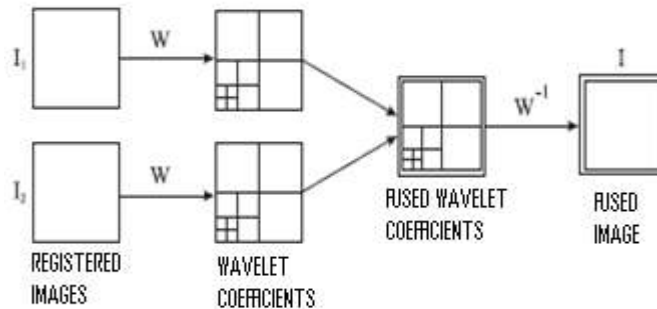


**FIGURE3:** Wavelet multi-dimensional fusion

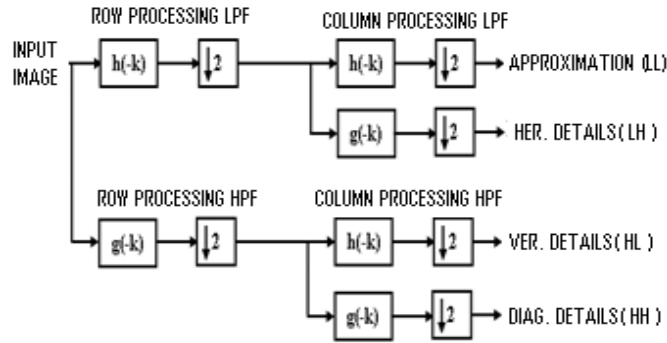


**FIGURE 4:** Two-dimensional orthogonal wavelet decomposition

**A. Wavelet based algorithm**

- 1) Apply wavelet transformation separately to each source image to establish various images of wavelet tower shaped transformation.
- 2) Fuse images at each transformation level.
- 3) Apply inverse Wavelet transform on fused wavelet pyramid.

In wavelet transformation due to sampling, the image size is halved in both spatial directions at each level of decomposition process thus leading to a multi-resolution signal representation. The decomposition and reconstruction of wavelet pyramid of source images are based on Mallet's theories. The most important step for fusion is the formation of fusion pyramid. It is difficult to decide a uniform standard for fusion principle. We applied the method to PET-MRI head image. We used mutual information based method for registering source images. In the process of fusion, we fused images at four different levels. In the next section, we make a quantitative evaluation of fusion at different levels.

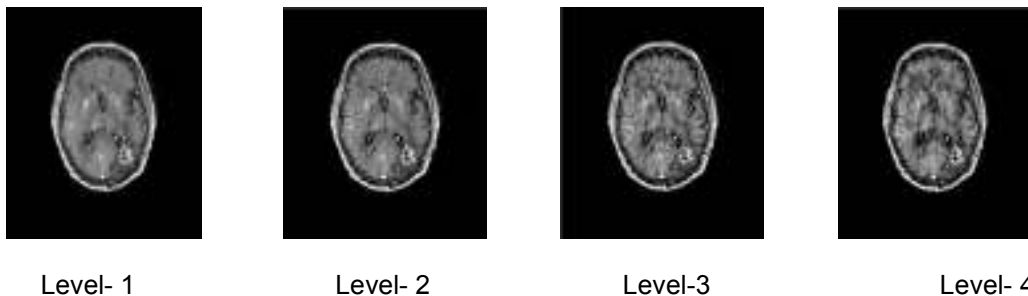


**FIGURE 5:** Wavelet based fused images at different levels

**Simple Average based Image Fusion**

This is a very basic technique of image fusion. Image fusion could be achieved by simple averaging corresponding pixels in each input image as follows

$$I_f(x, y) = \frac{I_1(x, y) + I_2(x, y)}{2} \dots \dots \dots (9)$$



FIGURE 6: Image fused by Averaging

### Image fusion based on Radon Transform

Radon transform is used to find linear features. Now a days, Houghs transform, Trace transform and Radon transform received much attention of researchers. Houghs Transform is a derivative of Radon transform and Radon transform is a special case of trace transform [24]. These three transforms are able to transform two dimensional images with lines into a domain of line parameters where each line in the image give a peak positioned at the corresponding line parameters. Radon transform of two dimensional function  $f(x,y)$  in  $(r, \theta)$  plane is defined as

$$R(r, \theta) = R[f(x, y)]$$

$$R(r, \theta) = \iint_{-\infty}^{\infty} f(x, y) \delta(r - x \cos \theta - y \sin \theta) dx dy \quad (10)$$

Where  $\delta(\cdot)$  is Dirac function,  $r \in [-\infty, \infty]$  is perpendicular distance of a line from the origine and  $\theta \in [0, \pi]$  is the angle formed by the distance vector with x-axis as shown in figure1.

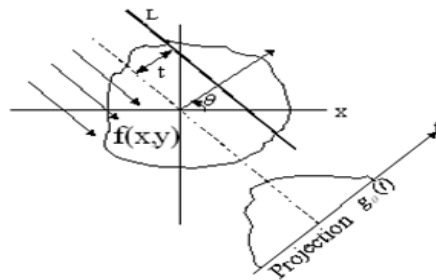


FIGURE7: Radon transform

### A. Image Fusion in Radon Space

Here we employed Radon transform for image fusion.

Algorirhm

- Register reference and sensed image.
- Compute Radon transform of both images.
- Take average of both images in radon space.
- Take inverse Radon transform.

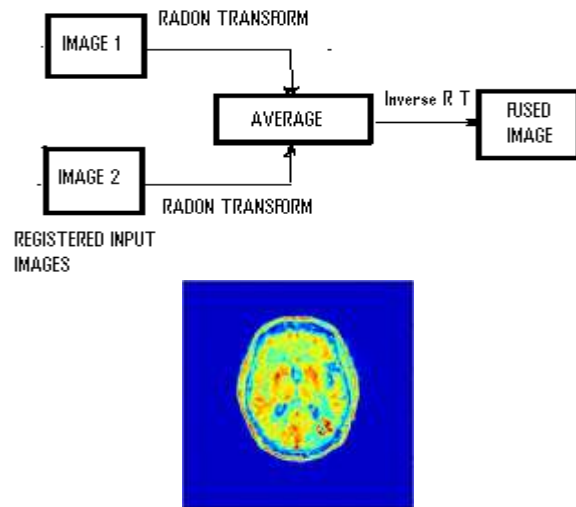


FIGURE 8: image fusion in Radon space and fused image.

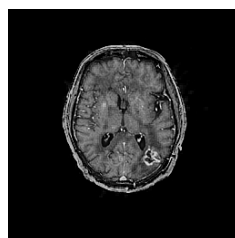
**Shift invariant discrete wavelet transform for image fusion**

The traditional DWT fusion encounters a number of shortcomings. It is well known that the DWT yields a shift variant signal representation resulting in a shift dependent fusion scheme. Fusion methods using DWT lead to unstable and flickering results. For the case of image sequences the fusion process should not be dependent on the location of object in the image and fusion output should be stable and consistent with original input sequence. SIDWT image fusion scheme overcomes this disadvantage. Considering some characteristic of the approximation wavelet coefficients of SIDWT, An approximation scale based wavelet coefficient maximum selection rule for image fusion was presented. Each stage of the SIDWT splits the input signal into the detail coefficient  $d_i(n)$ , and the approximation coefficient  $c_i(n)$  which serve as input for the next decomposition level

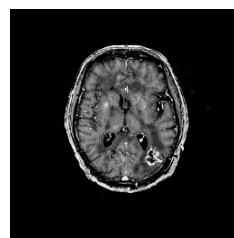
$$d_{i+1}(n) = \sum_k g(2^i \cdot k) \cdot c_i(n - k) \quad (11)$$

$$c_{i+1}(n) = \sum_k h(2^i \cdot k) \cdot c_i(n - k) \quad (12)$$

The decomposition start with  $c_0(n)=f(n)$ . The filter  $g(2^i \cdot k)$  and  $h(2^i \cdot k)$  at level  $i$  are obtained by inserting appropriate number of zeros between filter taps of the prototype filters  $g(k)$  and  $h(k)$ . The reconstruction of the input signal is performed by inverse SIDWT.



SIDWT level-2



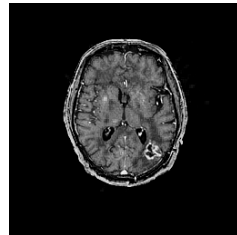
SIDWT level-4

**Laplacian Pyramids image fusion**

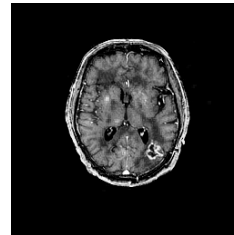
Laplacian pyramid of an image is a set of bandpass images, in which each is a bandpass filtered copy of its predecessor. Bandpass copies can be obtained by calculating the difference between



lowpass images at successive levels of a Gaussian pyramid. In Laplacian fusion approach the Laplacian pyramids for input images are used. A strength measure is used to decide from which source what pixels contribute at each specific sample location. For example, one can use the local area sum as a measure of strength. Following figure shows Laplacian Pyramid Fusion of PET and MRI image of brain. As can be seen for both tumor and anatomy of brain can be observed in the fused image.



Laplacian fusion level-2



Laplacian fusion level-4

### Contrast Pyramid /Ratio of Low Pass Pyramid

This section introduces a hierarchical image merging scheme based on multiresolution contrast decomposition. The composite images produced by this scheme preserve those details from the input images that are most relevant to visual perception. The essential problem in merging images for visual display is "pattern conservation": important details of the component images must be preserved in the resulting fused image, while the fusion process must not introduce spurious pattern elements that could interfere with succeeding analysis.

Contrast Pyramid is similar to the ratio of Low Pass Pyramid approach. Contrast itself is defined as the ratio of the difference between luminance at a certain location in the image plane and local background luminance to the local background luminance. Luminance is defined as the quantitative measure of brightness and is the amount of visible light energy leaving a point on a surface in a given direction.

The construction of the Contrast pyramid is similar to the construction of the popular Laplacian pyramid. First a Gaussian or low-pass pyramid is constructed. This is a sequence of images in which each image is a low-pass-filtered and subsampled copy of its predecessor. Let array  $G_0$  contain the original image. This array becomes the bottom or zero level of the pyramid structure. Each node of pyramid level  $l$  ( $1 \leq l \leq N$ , where  $N$  is the index of the top level of the pyramid) is obtained as a Gaussian weighted average of the nodes at level  $l-1$  that are positioned within a  $5 \times 5$  window centered on that node.

Convolving an image with a Gaussian-like weighting function is equivalent to applying a low-pass filter to the image. Gaussian pyramid construction generates a set of low-pass-filtered copies of the input image, each with a bandwidth one octave lower than that of its predecessor. The process that generates each image in the sequence from its predecessor is

$$G_l(i,j) = \sum_{m,n=-2}^2 w(m,n) G_{l-1}(2i+m, 2j+n) \quad \text{---(13)}$$

The weighting function  $w(m,n)$  is separable:  $w(m,n) = w'(m)w'(n)$ , where  $w'(0) = a$ ,  $w'(1) = w'(-1) = 0.5$ , and  $w'(2) = w'(-2) = a/2$ . A typical value of  $a$  is 0.4. Because we are primarily interested in merging images for visual display, we demand that visually important details of the component images be preserved in the resulting composite image. It is a well-known fact that the human visual system is sensitive to local luminance contrast. If an image fusion scheme is to preserve visually important details, it must exploit this fact. We now present an image decomposition scheme that is based on local luminance contrast. This scheme computes the ratio of the low-pass images at successive levels of the Gaussian pyramid. Since these levels differ in sample

density, it is necessary to interpolate new values between the given values of the lower frequency image before it can divide the higher frequency image. Interpolation can be achieved simply by following function

$$G_{i,k}(i, j) = 4 \sum_{m,n=-2}^2 w(m, n) G_{i,k-1}\left(\frac{i+m}{2}, \frac{j+n}{2}\right) \quad \text{---(14)}$$

At every level take ratio  $R_i$  of two successive levels. Luminance contrast is defined as

$$C = \frac{L - L_b}{L_b} = \left(\frac{L}{L_b}\right) - 1$$

Where  $L$  - luminance at certain location of image plane

$L_b$  - luminance of local background

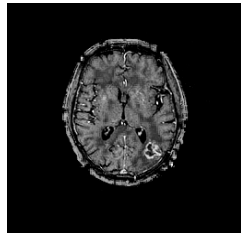
$I(i, j) = 1$  for all  $i, j$

$C_i = R_i - 1$

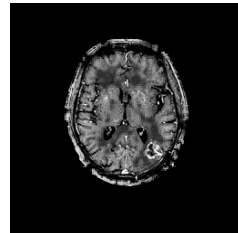
The image merging scheme can be cast into a three-step procedure. First, a ROLP pyramid is constructed for each of the source images. We assume that the different source images are in register and have the same dimensions. Second, a Ratio Of Laplace pyramid is constructed for the composite image by selecting values from corresponding nodes in the component pyramids. The actual selection rule depends on the application and may be based on individual node values or on masks or confidence estimates. For example, in the case of the fusion of two input images A and B into a single output image C and maximum absolute contrast as a selection criterion, we have, for all  $i, j$ , and  $l$

$$RC_l(i, j) = \begin{cases} RA_l(i, j), & \text{if } |RA_l(i, j) - 1| > |RB_l(i, j) - 1|, \text{ --- 15} \\ RB_l(i, j), & \text{otherwise,} \end{cases}$$

Here  $RA$  and  $RB$  represents contrast pyramids of two input images A and B and  $RC$  represents a fused image.



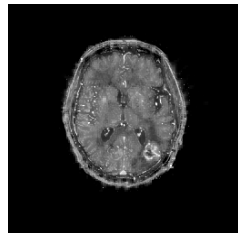
Contrast fusion level-2



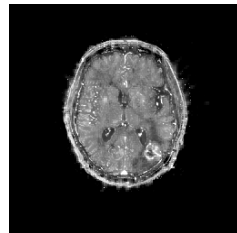
Contrast fusion level-4

**Ratio Pyramid**

Ratio of Low Pass Pyramid is another pyramid in which at every level the image is the ratio of two successive levels of the Gaussian pyramid.



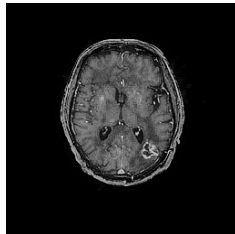
Ratio fusion level-2



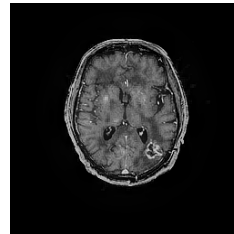
Ratio fusion level-4

### Filter-Subtract-decimate (FSD) Pyramid

FSD Pyramid technique is a more computationally efficient variation of the Gaussian Pyramid. This is similar to Laplacian fusion, the difference being in using FSD pyramid instead of Laplacian Pyramids. The only difference is in the step of obtaining the difference images in creating the pyramid. In Laplacian pyramid, the difference image  $L_k$  at level  $k$  is obtained by subtracting an image upsampled and then low-pass filtered at level  $k+1$  from the Gaussian image  $G_k$  at level  $k$ , while in FSD pyramid, this difference image is obtained directly from the Gaussian image  $G_k$  at level  $k$  subtracted by the low-pass filtered image of  $G_k$ . As a result, FSD pyramid fusion method is computationally more efficient than the Laplacian pyramid method by skipping an upsampling step.



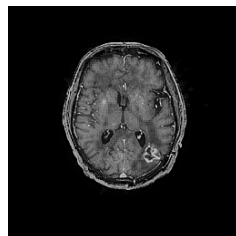
FSD Fusion level-2



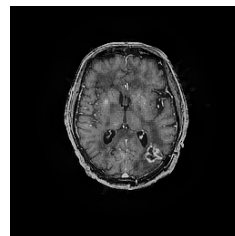
FSD Fusion level-4

### Gradient Pyramid

A gradient pyramid is obtained by applying a set of 4 directional gradient filters (horizontal, vertical and 2 diagonal) to the Gaussian pyramid at each level. At each level, these 4 directional gradient pyramids are combined together to obtain a combined gradient pyramid that is similar to a Laplacian pyramid. The gradient pyramid fusion is therefore the same as the fusion using Laplacian pyramid except replacing the Laplacian pyramid with the combined gradient.



Gradient fusion level-2



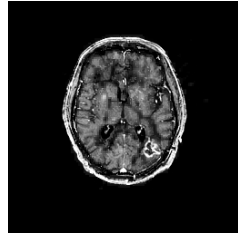
Gradient fusion level-4

### Morphological Pyramid

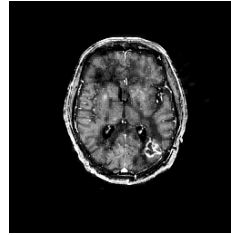
The multi-resolution techniques typically use low or bandpass filters as part of the process. These filtering operations usually alter the details of shape and the exact location of the objects in the image. This problem has been solved by using morphological filters to remove the image details without adverse effects. Morphological filters, composed of a number of elementary transformations like closing and opening transformations. The opening operator can be expressed as a composition of two other operators, erosion followed by dilation, both by the same input structural element. The main mechanism under the erosion operator is the local comparison of a shape, called structural element, Structuring element is a matrix used to define a neighborhood shape and size for morphological operations, including dilation and erosion. It consists of only 0's and 1's and can have an arbitrary shape and size. Morphological Pyramid Fusion method uses morphological pyramids instead of Laplacian or contrast pyramids.

A morphological pyramid is obtained by applying morphological filters to the Gaussian pyramid at each level and taking the difference between 2 neighboring levels. A morphological filter is usually for noise removal and image smoothing. It is similar to the effect of a low-pass filter, but it does not alter shapes and locations of objects in the image. The morphological pyramid fusion is

therefore the same as the fusion using Laplacian pyramid method except replacing the Laplacian pyramid with the morphological pyramid.



Morphological fusion level-2



Morphological fusion level-4

### 3.FUSED IMAGE EVALUATION

The purpose of multisensory fusion is to synthesize image data coming from different sensors into a single data set. Multi sensor image fusion is convenient and economical than designing the sensor with both resolution characteristics. Medical images from different sensors provide complementary information. Some applications require integration of such information. Doctors get anatomical knowledge from Magnetic Resonance Imaging (MRI) whereas physiological/functional knowledge from Photon Emission Tomography (PET). Image fusion can form a single composite image from different modality images of the same subject and provide complete information for further analysis and diagnosis. But it is necessary to align two images accurately before they fused. Before fusing images we should preserve all features in the images and should not introduce any artifacts or inconsistency which would distract the observer. Wavelet based fusion satisfies the requirement due to lots of advantages.

Image quality assessment plays an important role in medical applications. Image quality metrics are used to benchmark different image processing algorithm by comparing the objective metrics. There are two types of metrics that is subjective and objective used to evaluate image quality. In subjective metric users rate the images based on the effect of degradation and it vary from user to user whereas objective quality metrics quantify the difference in the image due to processing. The same dimension of image data is set for convenience in the fusion process and post-processing analysis. Before fusing the images they were registered. After registering, the fusion approaches- simple averaging, Principal component Analysis and wavelet based fusion at four different levels and Radon based fusion are used to create the fused images.

Assessment of image fusion performance can be first divided into two categories: one with and one without reference images. In reference-based assessment, a fused image is evaluated against the reference image which serves as a ground truth. Furthermore, fusion assessment can be classified as either qualitative or quantitative in nature. In practical applications, however, neither qualitative nor quantitative assessment alone will satisfy the needs perfectly. Given the nature of complexity of specific applications, a new assessment paradigm combing both qualitative and quantitative assessment will be most appropriate in order to achieve the best assessment result.

#### Assessment without Reference Images

In assessment without reference images, the fused images are evaluated against the original source images for similarity.

##### a. Entropy as a Quality Metric

Entropy is defined as amount of information contained in a signal. Shannon was the first person to introduce entropy to quantify the information. The entropy of the image can be evaluated as

$$H = -\sum_{i=1}^G P(i) \log_2(P(d_i)); \dots \dots \dots \langle 16 \rangle$$

Where G is the number of possible gray levels,  $P(d_i)$  is probability of occurrence of a particular gray level  $d_i$ .

Entropy can directly reflect the average information content of an image. The maximum value of entropy can be produced when each gray level of the whole range has the same frequency. If entropy of fused image is higher than parent image then it indicates that the fused image contains more information.

**b. Standard Deviation as a Quality Metric**

This metric is more efficient in the absence of noise. It measures the contrast in the fused image. An image with high contrast would have a high standard deviation.

$$\sigma = \sqrt{\sum_{i=0}^L \left( i - \bar{i} \right)^2 h_{I_f}(i), \dots \bar{i} = \sum_{i=0}^L i h_{I_f} \dots \dots \dots \langle 17 \rangle$$

Where  $h_{I_f}(i)$  is the normalized histogram of the fused image  $I_f(x,y)$  and L is number of frequency bins in histogram.

**c. Fusion Mutual Information as a Quality Metric**

It measures the degree of dependence of two images. A large measure implies better quality. If the joint histogram between  $I_1(x,y)$  and  $I_f(x,y)$  is defined as  $h_{I_1 I_f}(i,j)$  and  $I_2(x,y)$  and  $I_f(x,y)$  as  $h_{I_2 I_f}(i,j)$  then fused mutual information (FMI) is given as

$$FMI = MI_{I_1 I_f} + MI_{I_2 I_f} \dots \dots \dots \langle 18 \rangle$$

Where  $MI_{I_1 I_f} = \sum_{i=1}^M \sum_{j=1}^N h_{I_1 I_f}(i,j) \log_2 \left( \frac{h_{I_1 I_f}(i,j)}{h_{I_1}(i,j)h_{I_f}(i,j)} \right)$

$$MI_{I_2 I_f} = \sum_{i=1}^M \sum_{j=1}^N h_{I_2 I_f}(i,j) \log_2 \left( \frac{h_{I_2 I_f}(i,j)}{h_{I_2}(i,j)h_{I_f}(i,j)} \right)$$

**Assessment With Reference Image**

In reference-based assessment, a fused image is evaluated against the reference image which serves as a ground truth.

**a. Root Mean Square Error (RMSE)**

A commonly used reference-based assessment metric is the root mean square error (RMSE) which is defined as follows:

$$RMSE = \sqrt{\frac{1}{MN} \sum_{m=1}^M \sum_{n=1}^N (R(m,n) - F(m,n))^2} \dots \dots \dots \langle 19 \rangle$$

where  $R(m,n)$  and  $F(m,n)$  are reference and fused images, respectively, and  $M$  and  $N$  are image dimensions.

**b. Universal Image Quality Index ( UIQI)**

This measures how much of the salient information contained in reference image has been transformed into the fused image. The range of this metric is -1 to 1 and the best value 1 would be achieved if and only if reference and fused images are alike. The lowest value of -1 would occur when

$$I_f = 2 \mu_{I_r} - I_r$$

$$QI = \frac{4\sigma_{I_r I_f}(\mu_{I_r} + \mu_{I_f})}{(\sigma_{I_r}^2 + \sigma_{I_f}^2)(\mu_{I_r}^2 + \mu_{I_f}^2)} \quad (20)$$

Where  $\sigma_{I_r}^2$  Variance of reference image

$\sigma_{I_f}^2$  Variance of fused image

$\sigma_{I_r I_f}$  Covariance of reference and fused image

$\mu_{I_r}$  Mean of reference image

$\mu_{I_f}$  Mean of fused image

$$\mu_{I_r} = \frac{1}{MN} \sum_{i=1}^M \sum_{j=1}^N I_r(i,j)$$

$$\mu_{I_f} = \frac{1}{MN} \sum_{i=1}^M \sum_{j=1}^N I_f(i,j)$$

$$\sigma_{I_r}^2 = \frac{1}{MN - 1} \sum_{i=1}^M \sum_{j=1}^N (I_r(i,j) - \mu_{I_r})^2$$

$$\sigma_{I_f}^2 = \frac{1}{MN - 1} \sum_{i=1}^M \sum_{j=1}^N (I_f(i,j) - \mu_{I_f})^2$$

$$\sigma_{I_r I_f} = \frac{1}{MN - 1} \sum_{i=1}^M \sum_{j=1}^N (I_f(i,j) - \mu_{I_f})(I_r(i,j) - \mu_{I_r})$$

**c. Corelation coefficient**

The correlation coefficient measures the closeness or similarity in small size structures between the original and the fused images. It can vary between -1 and +1. Values close to +1 indicate that they are highly similar while the values close to -1 indicate that they are highly dissimilar. The ideal value is one when the reference and fused are exactly alike and it will be less than one when the dissimilarity increases.

$$CORR = \frac{2C_{rf}}{C_r + C_f} \quad (21)$$

Where

$$C_r = \sum_{i=1}^M \sum_{j=1}^N I_r(i,j)^2$$

$$C_f = \sum_{i=1}^M \sum_{j=1}^N I_f(i,j)^2$$

$$C_{rf} = \sum_{i=1}^M \sum_{j=1}^N I_f(i,j) I_r(i,j)$$

**d. Relative Mean**

The mean value of pixels in a band is the central value of the distribution of the pixels in that band. The relative shift in the mean value quantifies the changes in the histogram of the image due to processing. The relative shift in mean is defined as

$$relative\ mean = \frac{output\ mean - original\ mean}{original\ mean} \times 100\% \quad (22)$$

$$Relative\ mean = \frac{\mu_f - \mu_r}{\mu_r} \times 100\%$$

**4.RESULT**

**Data set 1 analysis**

In order to confirm the accuracy and validity of methods we have selected some sample images to carry on fusion experiment. Positron emission tomography (PET) can provide spatial information on metabolic activity in patients with cerebral glioma and functional data in patients with lesions closely related to eloquent brain areas. Because of the limited image resolution of PET, fusion with anatomic images such as MRI or CT is required to apply PET data for image guided surgery. The accuracy and clinical value of a novel image-fusion technique were evaluated for PET and MRI imaging modalities. We used the entropy of image to carry on appraisal. Table I gives the entropy of fused images and Table II shows Fusion Mutual Information.

s.n.	Method	Entropy	Mean	Std dev.
1.	Averaging	2.6333	149.6252	118.6502
2.	PCA	3.3793	23.5598	41.9296
3.	Wavelet level--2	3.3009	29.5368	57.3653
4.	Wavelet level--4	3.3653	29.9941	58.4344
5	Frequency domain	4.2764	44.6754	61.8042
6	Radon Transform	5.7492	48.5764	38.6664

7	Contrast Pyramid-level 2	2.6025	21.9640	44.1251
8	Contrast Pyramid-level 4	2.6408	23.0335	47.3534
9	FSD Pyramid-level 2	3.0847	23.4274	44.0464
10	FSD Pyramid-level 4	3.7630	24.1304	45.2177
11	Gradient Pyramid-level 2	3.0782	23.4990	44.1318
12	Gradient Pyramid-level 4	3.7470	24.2531	45.3556
13	Laplace Pyramid-level 2	2.7426	24.0742	47.7899
14	Laplace Pyramid-level 4	2.7414	26.2648	52.9269
15	Morphological Pyramid-level 2	2.9245	25.1721	52.5602
16	Morphological Pyramid-level 4	2.8756	26.1318	53.8263
17	Ratio Pyramid-level 2	2.9935	28.82	49.9349
18	Ratio Pyramid-level 4	3.0603	35.2122	60.6466
19	SIDWT with Harr level-2	2.8286	23.7187	45.8071
20	SIDWT with Harr level-4	2.7077	24.7476	50.0256

**TABLE I:** Entropy, mean and standard deviation values of fused images

s.n	Method	Combination	M.I.	FMI	Correlation Coef.	UIQI	MI	RMSE	Relative mean
1.	Simple averaging	PET-AVG <sub>f</sub>	3.0965	6.3490	0.8681	0.71153	3.4401	5.2267	0.0391%
		MRI-AVG <sub>f</sub>	3.2525						
2.	PCA	PET-PCA <sub>f</sub>	3.1002	6.2599	0.9109	0.9062	3.4355	5.2591	3.65%
		MRI-PCA <sub>f</sub>	3.1597						
3	Wavelet level-2	PET- W L2 <sub>f</sub>	3.2528	6.5465	0.8529	0.9234	3.2959	5.3566	0.81 %
		MRI- W L2 <sub>f</sub>	3.2937						
4	Wavelet level-4	PET- W L4 <sub>f</sub>	3.3392	6.7081	0.8227	0.7766	3.1840	5.4161	5.86 %
		MRI- W L4 <sub>f</sub>	3.3689						
5	Frequency domain	PET-FFT	2.7866	5.5280	0.8267	0.08397	3.2869	2.1895	1.5026 %
		MRI-FFT	2.7414						
6	Radon Transform	PET-RAD	2.5946	5.202	0.8058	0.0458	3.2597	1.9924	1.877 %



		MRI-RAD	2.607 9	5					
7	Contrast Pyramid-level 2	PET- CPL2	2.633 4	5.549 9	0.8458	0.9081	3.097 7	5.468 2	-6.70 %
		MRI- CPL2	2.916 5						
8	Contrast Pyramid-level 4	PET- CPL4	2.615 0	5.558 9	0.8368	0.9013	3.114 0	5.289 7	5.28 %
		MRI- CPL4	2.943 9						
9	FSD Pyramid-level 2	PET- FSDPL2	2.814 7	5.684 4	0.8637	0.9180	3.364 9	5.395 8	-0.50 %
		MRI- FSDPL2	2.869 7						
10	FSD Pyramid-level 4	PET- FSDPL4	2.788 2	5.650 5	0.8523	0.6930	3.302 4	5.414 8	2.50 %
		MRI- FSDPL4	2.862 3						
11	Gradient Pyramid-level 2	PET-GPL2	2.798 7	5.666	0.8651	0.9198	3.366 6	5.380 0	-0.21 %
		MRI-GPL2	2.867 3						
12	Gradient Pyramid-level 4	PET-GPL4	2.773 3	5.644 4	0.8542	0.7018	3.311 6	5.387 8	3.01 %
		MRI-GPL4	2.871 1						
13	Laplace Pyramid-level 2	PET- LPL2	2.715 7	5.566 4	0.838	0.9219	3.196 1	5.433 5	2.25 %
		MRI- LPL2	2.850 7						
14	Laplace Pyramid-level 4	PET- LPL4	2.614 9	5.417 5	0.842	0.9133	3.154 3	5.010 2	11.55 %
		MRI- LPL4	2.802 6						
15	Morphologica l Pyramid- level 2	PET-MPL2	2.798 9	5.613 1	0.7741	0.8915	3.301 4	5.516 9	6.92 %
		MRI-MPL2	2.814 2						
16	Morphologica l Pyramid- level 4	PET- MPL4	2.788 3	5.636 6	0.8032	0.8647	3.287 4	5.243 0	11.00 %
			2.848						

		MRI-MPL4	3						
17	Ratio Pyramid-level 2	PET- RPL2	2.8829	5.7168	0.8772	0.9160	3.3264	3.9722	22.42 %
		MRI- RPL2	2.8339						
18	Ratio Pyramid-level 4	PET- RPL4	2.8233	5.6038	0.8620	0.8775	3.3334	2.6324	49.57 %
		MRI- RPL4	2.7805						
19	SIDWT with Harr level-2	PET- SIDWTL2	2.7721	5.6319	0.8537	0.9200	3.2653	5.3939	0.72 %
		MRI- SIDWTL2	2.8598						
20	SIDWT with Harr level-4	PET- SIDWTL4	2.6290	5.3909	0.8313	0.9179	3.2068	5.3979	5.09 %
		MRI- SIDWTL4	2.7619						

**Table II:** Fusion Mutual Information, Cross correlation, UIQI, RMSE and Relative mean

**Data set 2 analysis**

In this data set, SPECT image with tumor and MRI image of same tumor of size 256 x 256 are considered for evaluation of the fusion algorithms. It can be seen that we get Physiological/functional knowledge from Single Photon Emission Computed Tomography (SPECT) while MRI gives anatomical information. Images are fused to have both types of knowledge simultaneously. Table III gives the entropy of fused images and Table IV shows Fusion Mutual Information.

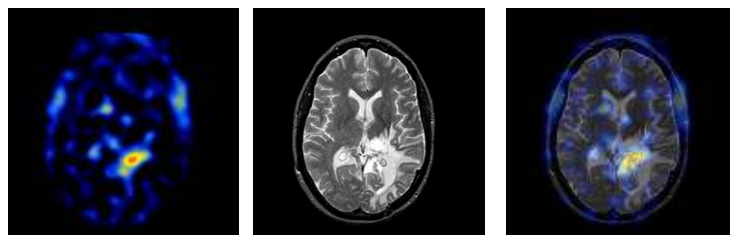


**FIGURE 11:** Sample images , SPECT (left ) and MRI (middle), reference fused image(right).

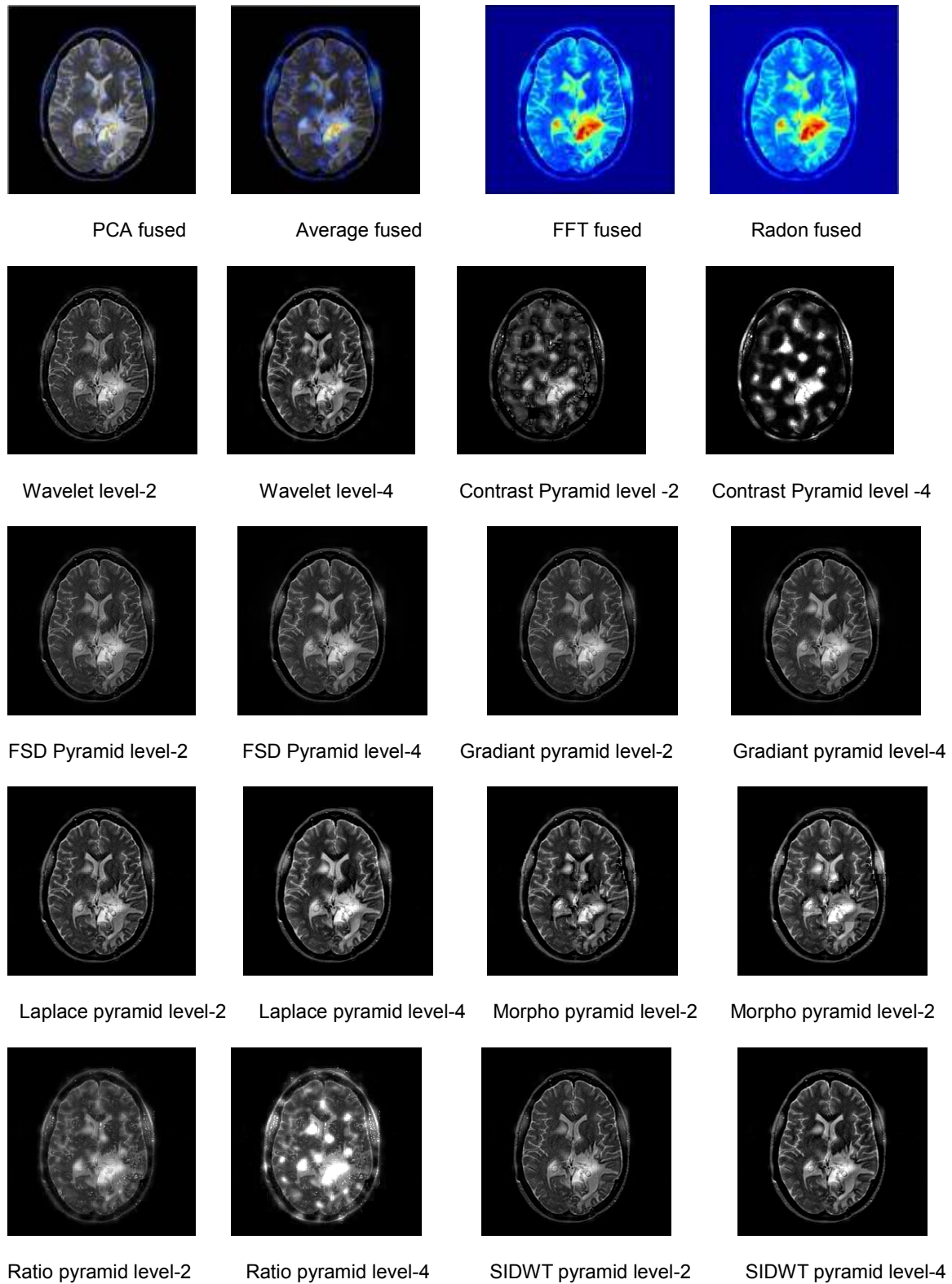


**FIGURE 12:** Images fused by different algorithms

s.n.	Method	Entropy	Mean	Std dev.
1.	Averaging	4.4555	28.4049	43.7129
2.	PCA	4.4275	35.6608	54.5568
3.	Wavelet level--2	4.9822	44.5692	55.1973
4	Wavelet level--4	5.2701	49.2849	48.1792
5	Frequency domain	5.0746	50.0557	53.9310
6	Radon Transform	4.9942	55.1852	56.3739
7	Contrast Pyramid-level 2	3.5883	19.2348	36.1107
8	Contrast Pyramid-level 4	3.4531	24.5718	39.7071
9	FSD Pyramid-level 2	4.2161	24.5201	38.5745
10	FSD Pyramid-level 4	4.5616	25.6973	40.2827
11	Gradient Pyramid-level 2	4.2117	24.5169	38.5974
12	Gradient Pyramid-level 4	4.4951	25.2924	39.8899
13	Laplace Pyramid-level 2	3.9182	25.1279	41.6786
14	Laplace Pyramid-level 4	3.7916	27.7533	47.6104
15	Morphological Pyramid-level 2	3.9905	24.5953	41.7123
16	Morphological Pyramid-level 4	4.0149	28.8634	48.7008
17	Ratio Pyramid-level 2	4.5316	29.2143	43.1095
18	Ratio Pyramid-level 4	4.7282	40.7323	60.0085
19	SIDWT with Harr level-2	4.0713	24.5718	39.7071
20	SIDWT with Harr level-4	3.7899	25.4521	43.6097

**TABLE III:** Entropy, mean and standard deviation values of fused images of dataset2

s.n.	Method	Combination	M.I.	FMI	Correlation Coef.	UIQI	MI	RMSE	Relative mean
1.	Simple averaging	SPECT-AVG <sub>f</sub>	2.7983	7.2706	0.715 1	0.4433	3.5121	6.7007	0.0419 %
		MRI-AVG <sub>f</sub>	4.4723						
2.	PCA	SPECT -PCA <sub>f</sub>	2.8556	6.7332	0.706 6	0.7886	3.5912	6.3073	-0.26 %
		MRI-PCA <sub>f</sub>	3.8776						
3	Wavelet level-2	SPECT - W L2 <sub>f</sub>	2.8851	6.708	0.690 8	0.9314	3.5286	6.1860	-.64 %
		MRI- W L2 <sub>f</sub>	3.8829						

4	Wavelet level-4	SPECT - W L4 <sub>r</sub>	2.8573	6.8999	0.671 5	0.7409	3.4754	6.8058	2.95 %
		MRI- W L4 <sub>r</sub>	3.8926						
5	Frequency domain	SPECT-FFT	2.8481	6.6918	0.693 8	0.0908	3.6194	4.747	1.024 %
		MRI-FFT	3.8437						
6	Radon Transform	SPECT-RAD	2.9007	6.709	0.686 2	0.0892	3.6081	3.7366	1.2318 %
		MRI-RAD	3.8083						
7	Contrast Pyramid-level 2	SPECT- CPL2	2.8603	6.576	0.606 6	0.8121	3.3272	0.6885	-22.2 %
		MRI- CPL2	3.7157						
8	Contrast Pyramid-level 4	SPECT- CPL4	2.7994	6.3806	0.478 6	0.6378	3.1999	6.6073	-23.30 %
		MRI- CPL4	3.5812						
9	FSD Pyramid-level 2	SPECT- FSDPL2	2.8051	6.6149	0.698 8	0.8744	3.4828	6.8316	-0.80 %
		MRI-FSDPL2	3.8098						
10	FSD Pyramid-level 4	SPECT- FSDPL4	2.8739	6.6985	0.697 2	0.6714	3.5207	6.8237	3.92 %
		MRI-FSDPL4	3.8246						
11	Gradient Pyramid-level 2	SPECT-GPL2	2.8254	6.5953	0.699 4	0.8765	3.4882	0.8309	-0.84 %
		MRI-GPL2	3.7699						
12	Gradient Pyramid-level 4	SPECT-GPL4	2.8571	6.6662	0.697 7	0.7533	3.4848	6.8504	2.30 %
		MRI-GPL4	3.8091						
13	Laplace Pyramid-level 2	SPECT- LPL2	2.7657	6.483	0.685 3	0.8268	3.4153	6.8536	1.61 %
		MRI- LPL2	3.7173						
14	Laplace Pyramid-level 4	SPECT- LPL4	2.7292	6.4592	0.681 6	0.8429	3.4098	6.6985	12.25 %
		MRI- LPL4	3.7300						
15	Morphological Pyramid-level 2	SPECT-MPL2	2.8011	6.4624	0.645 2	0.8018	3.3654	6.7190	-0.52 %
		MRI-MPL2	3.6613						
16	Morphological Pyramid-level 4	SPECT-MPL4	2.7988	6.6423	0.666 3	0.8598	3.4479	6.4851	16.74 %
		MRI-MPL4	3.8435						
17	Ratio Pyramid-level 2	SPECT- RPL2	2.9849	6.8625	0.688 2	0.8672	3.6130	6.1859	18.16 %
		MRI- RPL2	3.8776						
18	Ratio Pyramid-level 4	SPECT- RPL4	2.9843	6.9014	0.635 5	0.7024	3.5985	5.1827	64.96 %

		MRI- RPL4	3.9171						
19	SIDWT with Harr level-2	SPECT-SIDWTL2	2.8051	6.5549	0.692 2	0.8674	3.4567	6.8405	-0.60 %
		MRI-SIDWTL2	3.7498						
20	SIDWT with Harr level-4	SPECT-SIDWTL4	2.7540	6.494	0.682 7	0.8486	3.4254	6.8436	2.95 %
		MRI-SIDWTL4	3.7400						

**TABLE IV:** Fusion Mutual Information, Correlation coefficient, UIQI, RMSE, Relative mean

### 5.CONCLUSION

Image fusion is the process of image superposition using two different image types: anatomic (MRI) and functional (SPECT, positron emission tomography [PET]). This process provides the functional (SPECT antibody concentration) information in an anatomic context provided by the MRI image. It can be easy to see from the result obtained from both data sets that methods proposed in this paper have a very good effect. According to computation results, the increased entropy indicates the enhancement of information content. Approach of Radon transform provides more information as compare to other methods. But it is not clear from these results whether the enhancement of information contains more useful information or noise. From table I and III it is clear that image fusion in frequency domain and simple average contains high contrast while Radon based approaches shows a more amount of information as compared to other methods. Wavelet at level 4 shows a fair amount of contrast as well as entropy. Simple average is special domain method and produce special distortion while Fourier and Wavelet are transform domain fusions. PCA shows fair amount of entropy but contrast is not good. From table II and IV it is clear that Wavelet at level 4 shows a greater value of FMI even if Radon based approaches shows a more amount of information as compared to other methods.

Correlation coefficient was computed for different datasets. The correlation should be close to that of reference image to ensure good spectral quality. The values in the table II and IV indicate that the simple averaging and PCA method produces the best correlation result.

The histogram metrics, relative shift in mean and standard deviation, were computed. The relative shift in mean indicates the percentage by which the mean of the histogram has shifted. A positive value indicates a shift towards white and a negative value indicates a shift towards grey. The relative shift in mean values of the histogram is shown in the table II and IV for dataset 1 and dataset 2 respectively. In table IV ratio pyramid at level 2 and 4 shows 18 % and 65 % of shift respectively and in table II ratio pyramid at level 2 and 4 shows 22.42 % and 50 % shift respectively. In table IV contrast pyramid at level 2 and 4 shows -22 % and -23 % of shift respectively. This indicates a lot of distortion in the pixel values.

Table II and IV shows that fusion method based on simple averaging is least affected and wavelet, FSD pyramid, Gradient pyramid and SIDWT with Harr at level 2 are also affected less. Table II shows Root Mean Square Error value for dataset1. The values in the table indicates that the pixel values are less distorted in Radon based fusion and Frequency based method. But for dataset 2 RMSE shown in table IV indicate that pixel values are less distorted in contrast pyramid level 2 and gradient pyramid level 2.

Mutual Information between reference image and fused image also computed and it is observed that MI between reference and fused image is highest in simple averaging method for dataset 1 and ratio pyramid method for dataset 2 .are clearly visible. The simple averaging and PCA fusion

scheme leads to the best results in terms of mutual information. UIQI is highest in wavelet based method and is least in Radon based fusion.

The proposed fusion schemes were examined on two datasets .All fusion methods except Radon based fusion result in fused images of high contrast, all relevant objects of both input images are present in fused images. The SIDWT method resulted in a highly increased temporal stability of fused image sequence.

Many fusion algorithms have already been discussed to evaluate quality of fused image; however, these algorithms have not been assessed in terms of their visual performance. The visual performance-based assessment methodology is equally important. We evaluated the quality of a fused image by comparing its visual differences with the source images and which require no knowledge of the ground truth. It is observed that Wavelet at level-4 gives complete information with a better degree of contrast but at the cost of time. PCA and wavelet based fusion have been traditionally used for image fusion, but they have their own shortcomings. For PCA most information is gained if all calibrated and visually good quality multi-spectral input bands are used. PCA is general purpose approach and not application oriented. Wavelet based fusion can deal with images of different spectral and spatial resolutions. However, this method cannot handle cases where data is scattered or when input images differ greatly in either their spectral or spatial resolution. Figure 12 shows fused images of MRI image and SPECT image of brain with tumor. Brain tumor is clearly visible in SPECT image but not in MRI image . Figure shows that although single-photon emission computerized tomography (SPECT) provides unique functional information it is limited by poor anatomic detail. Non-specific localization of the antibody makes image interpretation difficult, since contrast improvement offered by SPECT imaging increases both the tumor specific and non-specific background uptake. Anatomy of brain can be observed in MRI image , not in SPECT image, but fused image shows anatomy of brain as well as tumor. The essential problem in merging images for visual display is “ pattern conservation”. Important details of the component image must be preserved in the resulting fused image; while the merging process must not introduce spurious pattern elements that could interfere with subsequent analysis. Laplacian decomposition scheme is based on local luminance differences. However, the human visual system is sensitive only to local luminance contrast. In the example of SPECT and MRI image if observers interest is in tumor then contrast pyramid is a better choice but if observers interest is in anatomy as well as tumor both, then SIDWT, yields good results. Researchers concluded that nonspecific antibody concentration in the blood pool or other normal anatomic structures is more easily recognized with MRI-SPECT or MRI-PET fusion due to the spatial overlay on structure. They also indicated that MRI-SPECT fusion was also useful in identifying tumor masses that were undetected on the MRI alone due to adjacent underfilled small bowels. The advantages of image fusion over visual comparison of multimodality are: (a) the fusion technique is useful to correct for variability in orientation, position and dimension; (b) it allows precise anatomic-physiologic correlation; and (c) it permits regional quantitation. Tumor volumes defined on the basis of antibody concentration can be generated from the SPECT images. The distribution of antibody uptake in specific anatomic regions or non-specific background regions can also be evaluated. Three-dimensional volumes of tumors of sufficient size can be generated and viewed from different spatial perspectives. Another important use of the registration-fusion technique is in follow-up studies where the primary purpose is to identify recurrence of the tumors or the spreading of metastatic disease. The major consequences of the fusion process is that the sites of suspected activity can be revisited post-surgery to determine the extent of recovery or recurrence of disease.

Future work includes more algorithms that combine aspect of pixel level and feature level fusion and more quality metrics to evaluate fused images.

## 6. REFERENCES

1. Brown Gottesfeld L., "Survey of Image Registration techniques", ACM Computing Surveys, 24, 4, and 1992, 325-376.
2. Barbara Zitova, Jan Flusser, "Image Registration Methods: A survey", Image and Vision Computing 21(2003)977-1000.
3. J.B. Antoine Maintz and Max A. Vierger , "A Survey of Medical Image Registration, Medical Image Analysis", (1/98) volume 2. number1, pp 1-37
4. Rafael C. Gonzalez, R. E. Woods, Stevan L. Eddins, *Digital Image Processing* (Pearson Education, 2003).
5. Haim Schweitzer, "Optimal Eigenfeature Selection by Optimal Image Registration," cvpr, pp.1219, 1999 IEEE Computer Society Conference on Computer Vision and Pattern Recognition (CVPR'99) - Volume 1, 1999.
6. Wen Cao; Bicheng Li; Yong Zhang, "A remote sensing image fusion method based on PCA transform and wavelet packet transform", Neural Networks and Signal Processing, 2003. Proceedings of the 2003 International Conference on 2:14-17 Dec. 2003 ,2: 976 - 981
7. Ma Debao Li Wugao Le Zhongxin Wang Jiefeng "The new matrix characteristic methods of image fine registration for synthetic aperture radar interferometry" Geoscience and Remote Sensing Symposium, 2000. Proceedings. IGARSS 2000. IEEE 2000 International, 2000, 2: 758-760
8. Du-Ming Tsai, Ron-Hwa Yang "An eigenvalue-based similarity measure and its application in defect detection" Image and Vision Computing , 23(12): 1094-1101, Nov 2005,
9. P.A. Van den Elsen, Evert-Jan D. Pol et al. "Medical Image Matching- a Review with Classification." IEEE Engineering Medicine and Biology, March , pp 26-38, 1993.
10. H. Li, B. S. Manjunath and S. K. Mitra "Multisensor Image Fusion Using the Wavelet Transform", Graphical Models and Image Processing. 57 (3): 235-245, 1995.
11. Zhao Zong-gui "An Introduction to Data Fusion Method." First press. 28<sup>th</sup> Institute of Electricity Ministry, 1998.
12. JIA Yong-hong, Li de-ren, SUN Jia-bing "Multidimensional Remote Sensing Imagery Data Fusion" Remote Sensing Technology and Application 2005, 15 (1) : 41-44.
13. David A Y "Image Merging and Data Fusion by Means of the Discrete Two Dimensional Wavelet Transform" J. Opt. Soc. Am. A, 1995 , 12 (9) : 1834-1841.
14. S. Mallat, "A Wavelet Tour of Signal Processing" Academic Press, Second Edition, 1998.
15. Svensson, J. R., M. O. Ulfarsson & J. A. Benediktsson, "Cluster Based Feature Extraction and Data Fusion in the Wavelet Domain" In: Pro. IEEE International Geoscience and Remote Sensing Symposium, pp. 867-869.
16. Garzelli, A "Possibilities and Limitations of the Use of Wavelets in Image Fusion." In: Pro. IEEE International Geoscience and Remote Sensing Symposium, 2002.
17. Lau Wai Leung, Bruce King and Vijay Vohora, "Comparison of Image Fusion Techniques using Entropy and INI", In: Pro. 22<sup>nd</sup> Asian Conference on Remote Sensing, 5-9 Nov 2001.



18. Chavez, P.S., Sides, S. C. Anderson, J.A., "Comparison of Three Different Methods to Merge Multiresolution and Multispectral Data: Landsat TM and SPOT Panchromatic", Photogrammetric Engineering and Remote Sensing, 57,295-303.
  19. Jiangsheng You, Weiguo Lu, Jian Li et. al. "Image Matching for Translation Rotation and Uniform Scaling by Radon Transform" 0-8186-8821-1/98, 1998 IEEE.
  20. Lau Wai Leung, Bruce King and Vijay Vohora, "Comparison of Image Fusion Techniques using Entropy and INI", In: Pro. 22<sup>nd</sup> Asian Conference on Remote Sensing, 5-9 Nov 2001.
  21. Rockinger, O., "Image Sequence Fusion Using a Shift Invariant Wavelet Transform," Proceedings of the International conference on Image Processing, 1997.
  22. Ramac, L. C., Uner, M. K., Varshney, P. K., "Morphological filters and wavelet based image fusion for concealed weapon detection," Proceedings of SPIE, 3376, 1998.
  23. Nunez, J., "Multiresolution-based image fusion with additive wavelet decomposition," IEEE Transactions on Geoscience and Remote Sensing, 37(3), 1999.
  24. Alexander Toet, van Ruyven, J.J. & Valetton, J.M., "Merging Thermal and Visual Images by a Contrast Pyramid", Optical Engineering, 28(7), pp. 789-792.
  25. Vivek Maik, Jeongho Shin and Joonki Paik, "Pattern Selective Image Fusion for Focus Image Reconstruction", Caip 2005, LNCS 3691, pp 677-684, 2005.
  26. Wen Doua, Yunhao Chen, "An Improved Image Fusion Method with High Spectral Fidelity", The International Archives of the Photogrammetry, Remote Sensing and Spatial Information Sciences. Vol. XXXVII. Part B7. Beijing 2008.
  27. Andrew P. Bradley, "Shift-invariance in the Discrete Wavelet Transform" Proc. VIIIth Digital Image Computing: Techniques and Applications, Sun C., Talbot H., Ourselin S. and Adriaansen T. (Eds.), 10-12 Dec. 2003, Sydney.
  28. Milad Ghantous, Soumik Ghosh and Magdy Bayoumi, "A Gradient-based Hybrid Image Fusion Scheme using Object Extraction", 2008 IEEE, 978-1-4244-1764-3/08.
  29. Toet, J. Van Ruvan, and J. Valetton, "Merging thermal and visual images by a contrast pyramid," Optical Engineering, 28, 1989.
  30. Alexander Toet, "Multiscale contrast enhancement with applications to image fusion", Optical Engineering 31(5), 1026-1031 (May 1992).
  31. P. Burt, E. Adelson, "Laplacian pyramid as a compact image code," IEEE Transactions on Communications, 31(4), 1983.
  32. Xydeas, C., and Petrovic, V., "Objective Pixel-level Image Fusion Performance Measure," Sensor Fusion: Architectures, Algorithms, and Applications IV, SPIE 4051:89-98, 2000.
-